NATURAL STATE MODEL OF KERINCI GEOTHERMAL SYSTEM, JAMBI, INDONESIA

Yudithia Prastika[1], John O'Sullivan[1] and Michael O'Sullivan[2]

[1]Geothermal Institute and Department of Engineering Science, University of Auckland, New Zealand

m.osullivan@auckland.ac.nz

Keywords: *Kerinci geothermal field, natural state, computer modelling*

ABSTRACT

The Kerinci geothermal system is located in Jambi Province, Indonesia. The study area is located on part of the Great Sumatra Fault which means it is a fault-controlled system. Many surface manifestations are found along the faults, such as steaming ground, fumaroles, hot springs and mud pools. The development of Kerinci is problematic as the Sikai area is situated in the Kerinci Seblat National Park in which all deforestation-related acitivities are banned. The geothermal prospect is controlled by Pertamina Geothermal Energy (PGE) who have recently drilled an exploration well.

In the present study a conceptual model was developed based on an analysis of information available in the literature. Then the conceptual model was used as the basis of a natural state, computer model of Kerinci. Manual calibration was used to improve the model by adjusting the model parameters, mostly the permeabilities, in order to obtain results corresponding to the conceptual model. However, the calibration process was difficult because little field data are available.

Finally the model was used to carry out production simulations to understand the behaviour of the system under unconstrained exploitation and to predict the sustainable production level of the Kerinci geothermal system. Overall, the production rate decreases over a 25 year production period (either the total mass flow rate or steam flow rate) accompanied by a gradual decline in pressure. On the other hand, the enthalpy is almost stable throughout the period.

1. INTRODUCTION

The Kerinci geothermal system is located in the Lempur area, Jambi Province, and mostly consists of volcanic rocks. Structurally, the system is classified as a fault-controlled system and there are two main faults dominating, namely Sikai Fault and Dua Belas Fault. The deep reservoir fluid is neutral chloride water with geothermometer-measured temperature of 220 – 260°C and there is an overlying vapor-dominated zone (JICA, 1989). Currently, the Kerinci geothermal prospect is being developing by Pertamina Geothermal Indonesia (PGE), one of the state-owned companies, managing the geothermal industry in Indonesia. Previously, two drilling investigations, to reveal the potential of the system, were conducted by VSI and JICA in 1983 and 1988, respectively. Recently, PGE has drilled and tested a deviated exploration well and categorized it as a successful production well. The well, KRC-B1, can deliver steam at 70 tonnes/hour and brine at 240 tonnes/hour with an enthalpy of 1100 kJ/kg, at a wellhead pressure of 5.5-6.55 bar (Silitonga, 2015). The KRC-B1 cluster was located outside the system boundary since, at present, the government forbids any activities inside the Kerinci Seblat National Park, which is acknowledged by UNESCO as a World Heritage Site.

The literature on the Kerinci geothermal system was reviewed and a conceptual model was developed. This conceptual model was used as the basis for a natural state computer model that was manually calibrated. The numerical simulator AUTOUGH2 (Yeh *et al*., 2012), the University of Auckland's version of TOUGH2 (Pruess, Oldenburg, & Moridis, 1999) was used for carrying out all the natural state simulations. To support the modelling, a graphical interface, TIM (Yeh *et al*., 2013), was used to visualise the results.

After a reasonable natural state model was obtained a number of future production simulations were carried out. Overall, the project was aimed at understanding the potential of Kerinci geothermal system under various types of exploitation scenarios and discovering the performance limit of the system.

2. CONCEPTUAL MODEL

2.1. Introduction

A conceptual model is created to achieve a good understanding of important aspects of the physical processes and structure of a geothermal system. The conceptual modelling approach is particularly effective when exploring blind prospects because it makes fuller use of limited data and helps to identify strategies for addressing the lack of information, as well as identifying targets (Cumming, 2009). There are some vital components for a conceptual model of a potential geothermal area, namely: heat source, reservoir structure (e.g., good permeability, lithologically or structurally determined), recharge fluids, and discharge zones (thermal signatures) (Utami, 2015).

Kerinci geothermal field is located in the Lempur village area which is approximately 10 km southeast of Kerinci Lake, roughly 30 km south east of Sungai Penuh town, and approximately 525 km from Jambi Capital City (10 hour drive). The Lempur site is at an elevation of about 1400 m above sea level. The Kerinci geothermal field has been under development by Pertamina Geothermal Energy (PGE) since 2008 (Silitonga *et. al*., 2015).

To build a conceptual model, all field data related to the area were compiled and analysed. The published data on the Kerinci geothermal area are limited, yet they are sufficient to build a conceptual model. They include geology, geophysics, geochemistry, and data from existing exploration wells. There are three exploration wells in the Kerinci geothermal system, located in the eastern Mt. Kunyit, Lempur area. Two wells were drilled by JICA jointly with VSI. The first well, LP-1, drilled in 1983 and the second, LP-2, drilled in 1988 are separated by 1.5 km. The third well, KRC-B1, was drilled by Pertamina in July

2007. This well is deviated with a 50^0-65^0 inclination and penetrates to a measured depth of 2650 m, with a maximum horizontal displacement of 1650 m and vertical depth of 1899 m.

2.2. Geology

Kerinci is located in Sumatera Island, one of the biggest islands in Indonesia. Figure 1 shows the area of this study. In the west part of Indonesia, the Indian Ocean Plate is subducting beneath the Southeast Asia Plate. Because of the movement of the plates, there is large-scale strike-slip fault forming inside the island. The fault is a dextral strike-slip fault and can be traced for about 1660 km. Many observations have been undertaken to assess the rate of slip of this fault and GPS (Global Positioning System) measurements indicate that the largest tectonic movement, of 24 mm/yr, occurs in north western Sumatra and the smallest, of 6 mm/yr, in south eastern Sumatra (McCaffrey, 1991; Bellier and Sébrier, 1995; Genrich *et al.*, 2000; McCaffrey *et al*., 2000; Prawirodirdjo *et al*., 2000). Satellite image analysis (Bellier and Sebrier, 1995) showed that some calderas have evolved from pull-apart basins. Hochstein and Sudarman (1993) said that the huge potential of high-temperature geothermal resources in Sumatra is associated with the Sumatran Fault and many of these geothermal fields are situated in the pull-apart basins (Hickman *et al*., 2004).

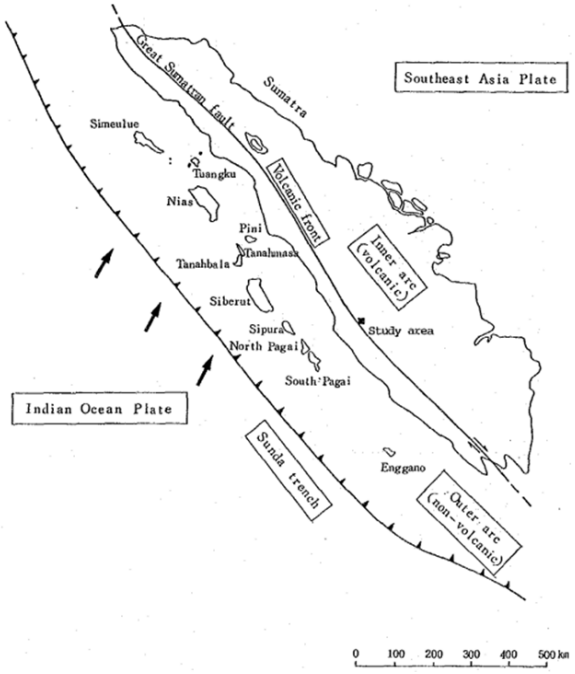

Figure 1: The location of the study area in Sumatra Island.

There is a high geothermal potential in the depression zone because there is highly active magmatism resulting from plate subduction (JICA, 1989). As has been noted, the area of the present study, Kerinci, is one of the areas located in this depression zone and is situated in the 70 km long Siulak segment (2.25^0 S to 1.7^0 S).

The study area is mainly covered by Quaternary volcanic rocks comprised of three main formations including: Tua volcanic rocks, Raja volcanic rocks, and Kunyit volcanic rocks, as shown by Figures 2 and 3. In the flat terrain, fan deposits can also be found and alluvium is widely distributed in the northern part. A few outcrops from the basement Tertiary and Mesozoic can be identified in this area as they are distributed under the Quaternary volcanic rocks. The Mesozoic rock group is composed of grey, hard limestones, often in association with lenticular shale beds (Hasri, 1984). It is also noted that this group is associated with the Barisan Formation while the Tertiary system consists of basaltic andesites and acidic volcanic rocks, mainly rhyolites and dacites.

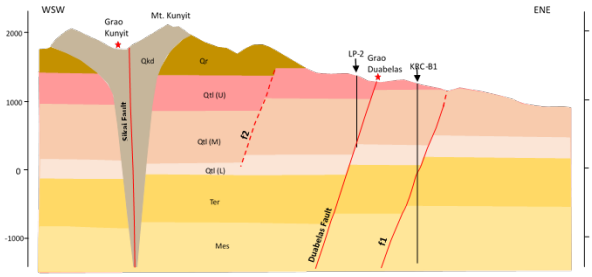

Figure 2: Geological Cross section from ENE to WSW

Above the basement rocks, Pleistocene formations are present, consisting of three main volcanic rocks. First are the volcanic rocks whose deposition age is in the early Pleistocene, for example, the Tua volcanic rocks, that are strongly altered and rich in joints. After that, there are the Raja volcanic rocks which are relatively young and lie above the Tua volcanic rocks. Lava flows and tuff breccia characterize the area. In general, the character of this rock type is similar to the Tua volcanic rocks which are dominantly jointed. Thirdly, Kunyit volcanic rocks lie above the Raja volcanic rocks and form the Kunyit lava domes, Kering lava, Lempur pyroclastic flow, and Rawang-Sipedjani pumice gravel bed. The lava domes are basically of pyroxene-hornblende type, formed in the upper Pleistocene. The Lempur pyroclastic flow mainly consists of pyx-ho dacitic volcanic breccia and ash bed whereas Rawang-Sipedjani is composed of dacitic pumice and silt and is thought to have resulted from sedimentation in water (JICA, 1989).

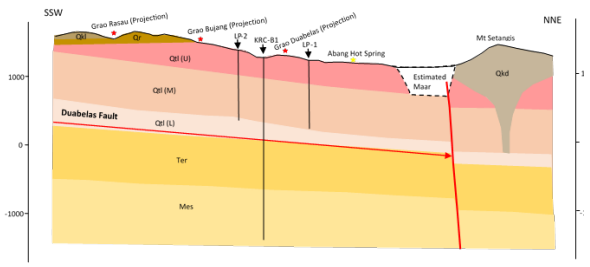

Figure 3: Geological Cross section from NNE to SSW

Figure 4 shows that there are several faults dominating the area. In general, NW-SE and NNE-SSW trending faults are clear. The review by Hasri (1984) suggests that the NW-SE faults are part of the Great Sumatra Fault zone and can be viewed running parallel to the Barisan Mountain Range. The manifestations, shown in Figure 4, mostly emerge along the faults.

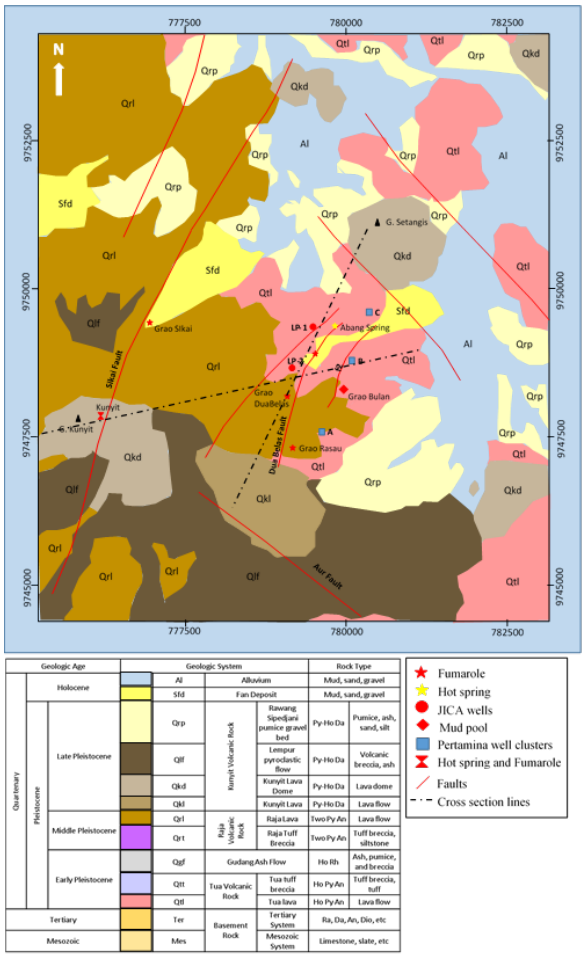

Figure 4: Plan view of the Kerinci geothermal area, its formations and surface features

The two fault zones controlling the manifestations are the Sikai Fault zone and Dua Belas Fault zone. These two faults have a similar NE-SW trend. There are also some faults in the NW-SE direction which are highly correlated and parallel with part of the fault segment of the GSF. However, along these faults, manifestations are rare, especially for the faults located to the northeast of the area.

The NNE-SSW and NW-SE faults can be interpreted as reflecting the strain field caused by the activities of the Great Sumatra Fault zone (Hasri, 1984). However, there is a lack of information about the character of these faults.

2.3. Geochemistry

As previously mentioned, in the study area, the manifestations tend to appear along the faults. Some of the locations observed are at Grao Sikai and Garo Kunyit in the Sikai area (on the Sikai Fault) and at Grao Duabelas, Grao Bujang, Grao Rasau, Grao Bulan, and Abang hot spring in the Duabelas area (near the Duabelas fault complex). However, to the southeast of Mt. Kunyit, the Kering alteration zone occurs on the Aur Fault, but is associated with no active thermal features. Silitonga *et al.* (2015) observed that the alterations in the nearby manifestations are argillic alterations (smectite) and they also found minor amounts of sulphur deposits in Grao Sikai. Their observations agree with statements in the JICA report that the occurrence of kaolinite and/or alunite (argillic group) result from acidic hot water.

In Grao Kunyit, while hydrothermal alteration extends widely to the surrounding the fumaroles, it is relatively narrow in Grao Sikai. Abang hot springs discharge 60°C water and there is a lack of an alteration zone. At the Grao Bulan fumaroles area, the extent of the hydrothermal alteration is narrow while in Grao Duabelas, Grao Bujang and Grao Rasau, there are intensive fumaroles and boiling mud pools accompanied by a vast alteration zone. Analysis of isotope ratios of hydrogen and oxygen from the Duabelas fumaroles area indicate that their steam is derived from a vapour dominated zone which is the product of a deep boiling reservoir. The temperature of this zone is estimated to be 135°C to 160°C. On the other hand, neutral bicarbonate type hot water is flowing out at the Abang hot springs which results from percolation of the upflowing steam into the groundwater aquifer, producing an estimated temperature of 145°C to 168°C (JICA, 1989).

The chemical composition of LP-1 has been analysed and it shows that the geothermal system is of a neutral chloride type and the estimated temperature based on isotope analysis is in the range 200 – 300°C. The LP-2 drilling record shows the reservoir fluids are of meteoric origin and are of chloride type, similar to LP-1. Yet, from silica and Na-K-Mg thermometers, the estimated deep reservoir temperature is higher than in LP-1, at approximately 220°C and from fluid inclusion measurements is about 224°C. However, the isotope geothermometer identifies higher temperatures, ranging from 238°C to 271°C.

Different conditions were discovered in the Sikai area, with barely any water found discharging that could be used to assess the reservoir temperature. However, since the chemical composition of fumarolic gas in Sikai is similar to that at Duabelas, it can be concluded that the Sikai area is of the same neutral chloride type and the reservoir fluid emanates from a common source. Nonetheless, a gas isotope thermometer indicates a higher temperature than in the Duabelas area, of not lower than 261°C.

2.4 Geophysics

There are a few published geophysical investigations of this area, namely: a resistivity investigation which was done in the 1980's and MT and gravity surveys conducted in 2007 by Pertamina. However, there is a lack of detailed information about the two newest studies. For example, there is no cross section showing MT resistivity distribution in the sub-surface.

Resistivity data were derived from 75 vertical soundings with a Schlumberger array with distances of up to AB/2=1000 m. There are four survey lines (A, B, C, and D) covering an area of about 22 km^2 over the northern slopes of Mt. Kunyit, as shown in Figure 5. Two maps which were produced include an iso-resistivity map and a sounding map. An overview of the apparent resistivity structure of the survey area is given by the apparent resistivity maps, for AB/2= 500 m and AB/2= 1000 m, shown by Figure 7 (A) and (B). It can be seen that the low resistivity ground is associated with Grao Bujang, Grao Duabelas, and Abang hot spring. Another low resistivity area also occurs over the Grao Sikai thermal area on the northern slopes of Mt. Kunyit.

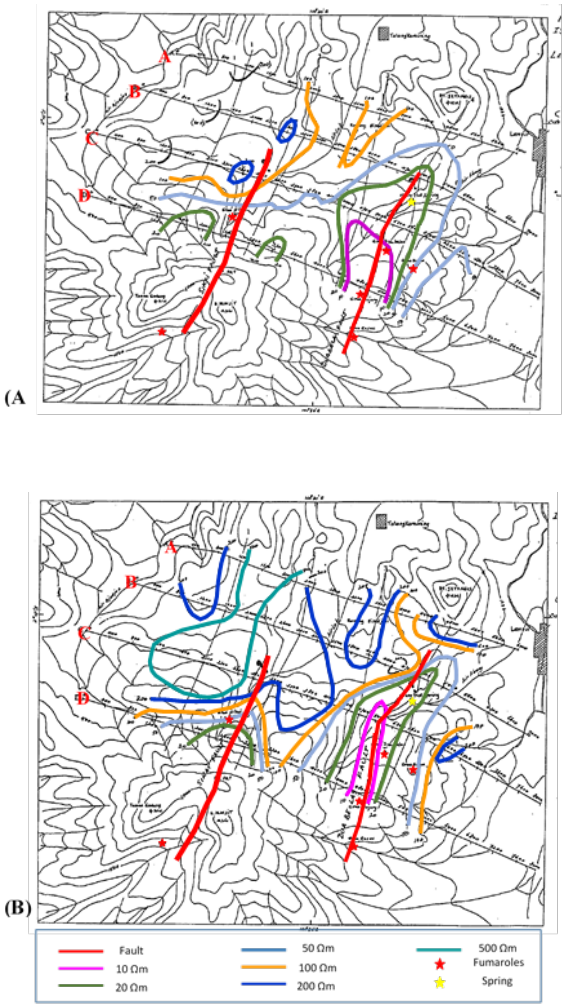

Figure 5: The iso-resistivity maps of the Lempur (Kerinci) geothermal system measured by JICA and analysed by Hasri (1984). (A) is the iso-resistivity map with AB/1000 m and (B) is the iso-resistivity map with AB/500 m

To understand the vertical resistivity structures, pseudo-resistivity maps, from which are plotted the apparent resistivity versus an apparent depth, were produced for lines A, B, C, and D (not shown). The plots show that beneath lines A and B, there are higher apparent resistivities than beneath lines C and D. This situation applies in the most western and most eastern part of line D, while in the middle we can find an intense low resistivity which may be related to thermal alteration of rocks.

Hasri (1984) was suspicious of the interpretation of the vertical results produced by JICA because he detected some peculiar anomalies caused by EM coupling effect. He reprocessed the JICA data and then reinterpreted the results. The comparison for line D is shown in Figure 6 (1) and (2). The pseudo-resistivity, beneath line B, C, and D shows there are low resistivity rocks near the Sikai Fault and the Duabelas Fault. Assuming that low resistivity is mainly caused by thermally altered rocks, the alteration is thicker beneath line D than line A.

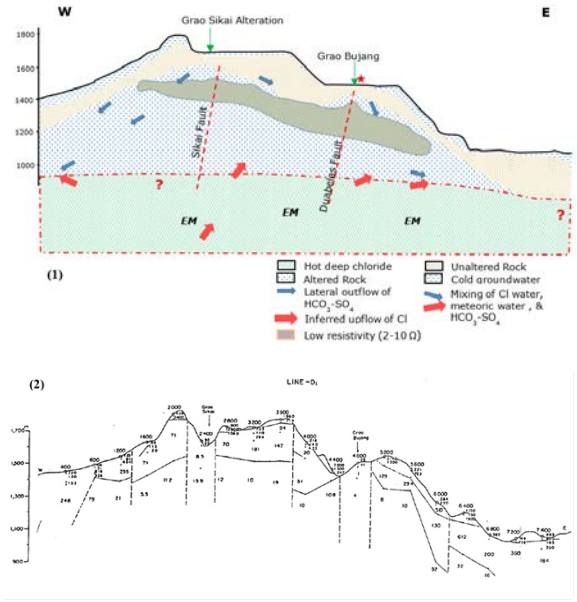

Figure 6: The sounding maps of resistivity investigations in the Kerinci geothermal area. (1) is the modified 're-interpretation map' from Hasri (1984) and (2) is the map produced by JICA (1983)

In 2007, there were more geophysical investigations of the study area. Silitonga *et al.* (2015) described two geophysical surveys using magnetotelluric and gravity methods. However, in the published paper, there are no detailed analyses to delineate the subsurface. Silitonga *et al.*, (2015), from a Bouguer anomaly map, detected a low density anomaly zone (-20 mGal) close to Mt. Kunyit and correlated to the alteration zone. A resistivity map produced from the MT method reveals that the conductive clay cap (<10 ohmm), interpreted as the smectite zone, is located in the eastern of part of the prospect, near Mt. Kunyit. This conductive layer is relatively thin (less than approximately 700 m), overlying the slightly resistive layer that is estimated to form the reservoir.

2.5 Final Conceptual Model

All available geoscientific data related to the Kerinci geothermal system were discussed above. The data were integrated to build a comprehensive conceptual model of Kerinci. Figure 7 and 8 display two vertical sections through the conceptual model, directed ENE-WSW and NNE-SWS, intersecting the Sikai and the Dua Belas Fault.

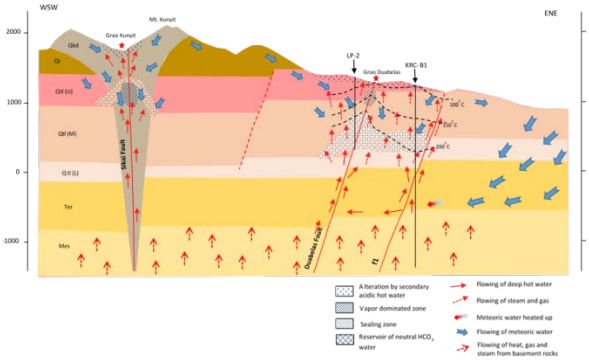

Figure 7: Conceptual model of the Kerinci geothermal system. ENE-WSW cross section

The colours represent the lithology units, blue and red arrows show cold fluids penetrating down and heated fluids (reservoir fluids) flowing up to the surface, respectively. Also shown are surface manifestations, wells, estimated temperatures and the location of the clay cap.

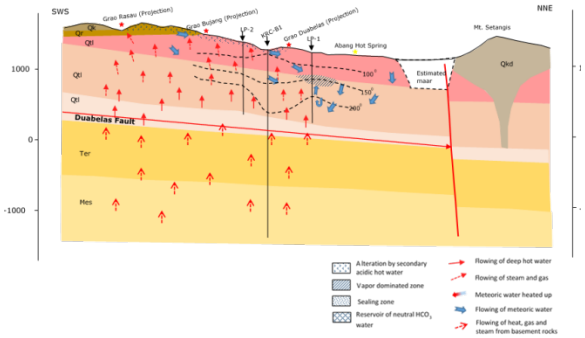

Figure 8: Conceptual model of the Kerinci geothermal system. NNE-SWS cross section

3. COMPUTER MODEL

3.1 Model Description

A regular rectangular grid is used for the model. The area of the grid is 16 km x 14 km and it is divided into an outer area and an inner area. The outer area blocks are 1 km x 1 km in size and the inner area has a better resolution with 500 m x 500 m blocks. Vertically, the model is set up with 19 layers. Layer 0 is the atmospheric layer and layers 1 to 19 are for rock lithology units. Layers 1 to 15 are set to be 200 m thick and the rest of them are 500 m thick. Layers 16 to 19 represent the basement and so they have uniform lithology. The elevation of the top of the model follows the topography.

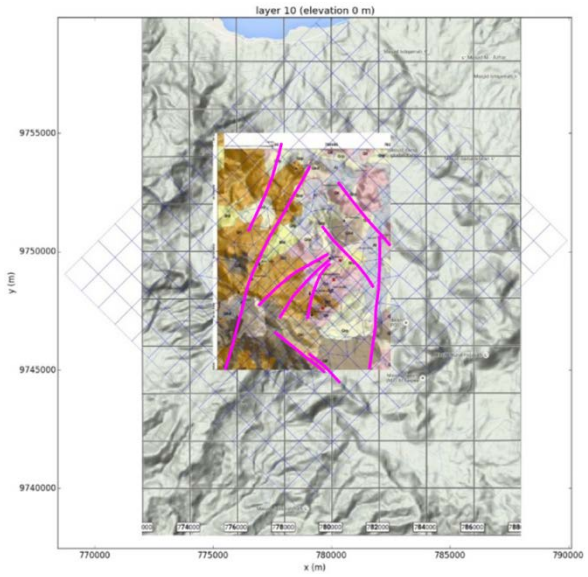

Figure 9: The model grid, the topography and geological map. Faults are shown in magenta.

The total number of blocks is approximately 7000. Figure 9, above, shows the topographical map, overlaid by a geology map and by the model grid.

The red dots and green square in Figure 10, a plan view of the grid, correspond to the surface features and KRC-B1 (Pertamina well), respectively. Figure 11 is a vertical cross section showing the layer structure.

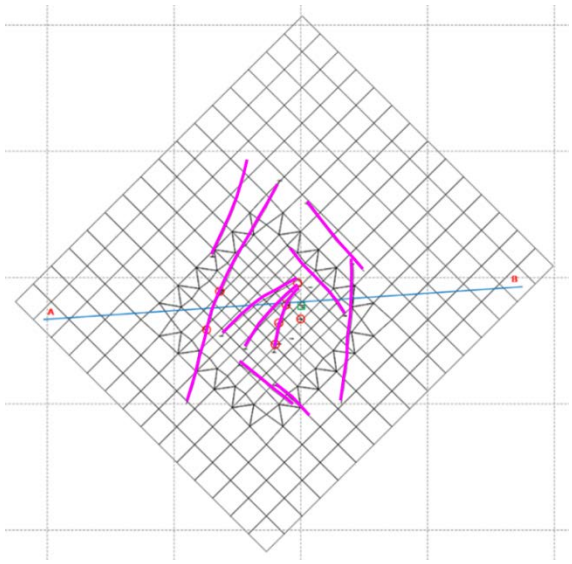

Figure 10: Plan view of model showing faults (magenta), surface features (red dots), and a well (green square)

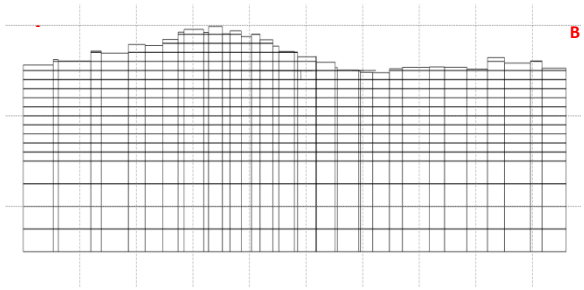

Figure 11: Layer structure for model on section AB.

Table 1: Lithological units and parameter values

No	Rock name	Geologic system	Permeability		
			k1	k2	k3
1	A0001	Alluvium	4E-16	5E-16	4E-16
2	B0001	Fan Deposit	4E-16	5E-16	4E-16
3	C0001	Kunyit Volcanic Rock (pumice gravel)	4E-16	5E-16	4E-16
4	D0001	Kunyit Volcanic Rock (pyroclastic flow)	4E-16	5E-16	4E-16
5	E0001	Kunyit Volcanic Rock (lava dome)	4E-16	5E-16	2E-16
6	F0001	Kunyit Volcanic Rock (lava)	4E-16	5E-16	4E-16
7	G0001	Raja Volcanic Rock (lava)	1E-16	2E-16	2E-16
8	H0001	Tua Volcanic Rock (tuff breccia)	4E-16	5E-16	4E-16
9	T0001	Tua Volcanic Rock (Upper)	2E-16	2E-16	2E-16
10	U0001	Tua Volcanic Rock (Medium)	2E-16	2E-16	2E-16
11	V0001	Tua Volcanic Rock (Lower)	2E-16	2E-16	2E-16
12	I0001	Basement Rock	5E-16	5E-16	5E-16
13	J0001	Basement Rock	5E-16	5E-16	5E-16

The lithology and the permeability structure were set up based on the geological map and conceptual model. The initial lithology units and their initial permeability values are shown in Table 1.

There are, in addition, 10 faults identified in the Kerinci geothermal system, as shown in Table 2. The locations of the faults (listed in Table 2 and shown in Figure 10) were based on two maps, namely: Pertamina literature (2015) and JICA map (1989). However, the fault properties, such as dip, azimuth etc. could not be determined properly due to lack of information and so they were treated as vertical. This enabled the model blocks corresponding to each fault to be identified using the fault traces and then new "faulted" rock types to be assigned to each block. Thus faulted rock types were created for each of the faults in each of geologic systems listed in Table 1. The faulted rock types were distinguished from their base lithology by the assignment of different rock properties in terms of permeability, porosity, etc. The basic idea behind this approach is that since a fault can act as a conduit or as a barrier, each fault should be assigned unique parameters that either enhance or retard flow as a result of the faulting. Table 2 also shows how this approach has altered the permeabilities of the Basement rock type (I0001).

Table 2: Faults used in the model with permeabilities given for the Basement rock type (I0001)

No	Fault Name	Direction	Permeability (Basement)		
			k1	k2	k3
-	No Fault	-	5E-16	5E-16	5E-16
1	Fault 1	NE-SW	1E-16	5E-16	2E-15
2	Fault 2	NE-SW	5E-16	2E-15	2E-15
3	Fault 3	NNE-SSW	5E-16	5E-16	2E-15
4	Fault 4	NW-SE	1E-15	1E-16	5E-16
5	Fault 5	NNE-SSW	2E-16	2E-16	2E-15
6	Fault 6	NW-SE	5E-16	1E-16	1E-15
7	Fault 7	NNW-SSE	1E-15	1E-15	1E-15
8	Fault 8	NNW-SSE	5E-16	5E-16	2E-15
9	Fault 9	NW-SE	5E-16	1E-16	2E-15
10	Fault 10	NNE-SSW	2E-16	2E-16	2E-15

The important matters related to building a model are, first, the size and structure of model, and then second are the boundary conditions. The boundary conditions for this model are as follows:

- The top boundary was assigned an atmospheric pressure of 1 bar and temperature of 25^0 C. The surface lithology units are assigned a high permeability to allow simulation of the correct the position of the water table. Some modellers have used a flat water table while others have adjusted the thickness of the top blocks of the model to match the variable elevation of the water table (O'Sullivan *et al.*, 1998).
- The side boundaries are assumed to be closed to heat and fluid flow;
- Most of the bottom boundary was assigned a constant background heat flux of 0.08 W/m^2 while some blocks were set up to be the locations of hot mass recharge, as shown in Figure 12. The total flow rate of recharge is 35 kg/s with an enthalpy of 1300 kJ/kg.

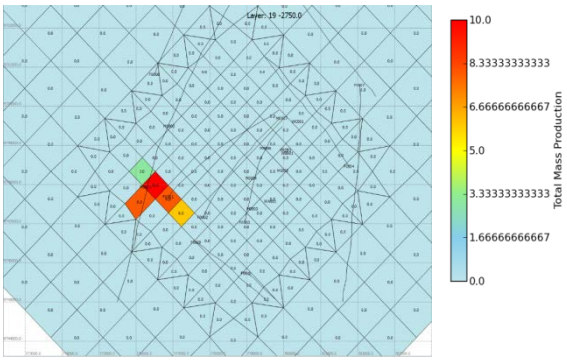

Figure 12: Mass recharge blocks at base of the model

The structure of permeability in the Kerinci geothermal model is focused on the faults since they are the reason why the heated fluids in the reservoir appear at the surface. They act as channels for hot fluids to seep out of the system. Also, some of the faults act as conduits for water from natural precipitation to recharge the geothermal system. Thus the faults have two roles generally, as an entrance and an exit for the fluids. All of the structures are assumed to extend to the basement.

The rock properties for the faults are assigned differently from the rock properties in the background formations (as given in Table 1). It is expected that most faults will act as conduits and should have high permeability and porosity. However a few faults may act as barriers and should have low lateral permeability. The details were determined by calibration.

3.2 Model Calibration and Results

By using the numerical simulator, AUTOUGH2, a natural state model was generated and calibrated to match the field data and the conceptual model. It was necessary to make several adjustments to the model during the calibration phase to achieve a good match with the real system. The variables that were modified were: the permeability (both horizontal and vertical), the deep upflow of mass at the lowermost layer, the thickness of surface lithology and the clay cap settings. Some small adjustments and re-interpretations in lithology or structures were also made. Figures 13 and 14 show the structure of the natural state model and Figures 15 and 16 show the temperatures on the same profiles.

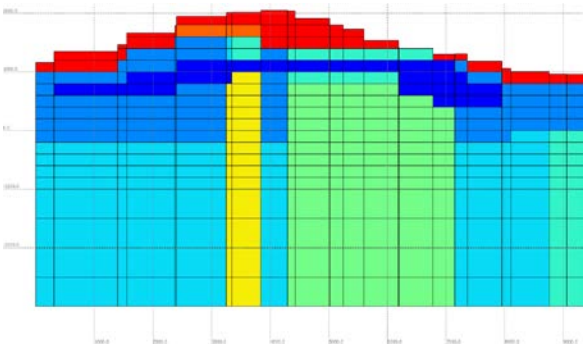

Figure 13: Vertical permeability on ENE-WSW vertical slice of the calibrated natural state model.

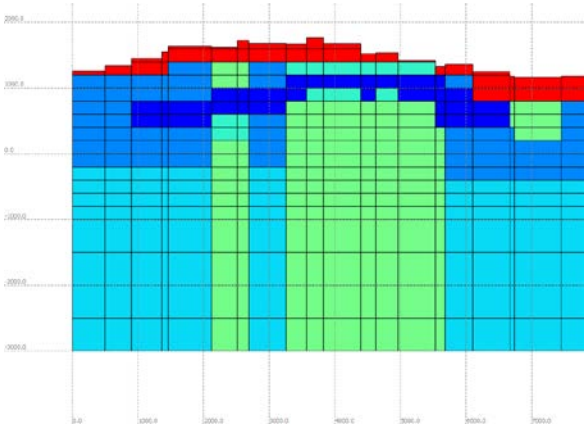

Figure 14: Vertical permeability on NNE-SSW vertical slice of the calibrated natural state model.

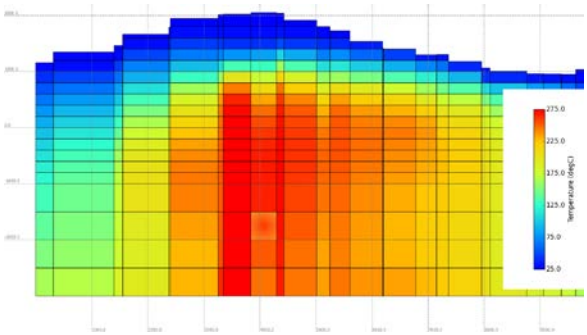

Figure 15: Temperatures on an ENE-WSW vertical slice through the calibrated natural state model.

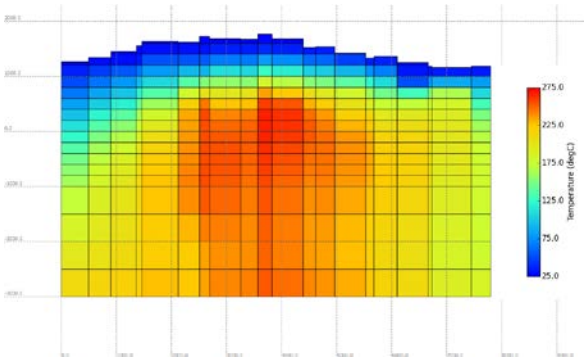

Figure 16: Temperatures on a NNE-SSW vertical slice through the calibrated natural state model.

The final calibrated model reasonably reflects the conceptual model. Similar temperatures are shown in the natural state model, especially the temperatures beneath Mt. Sikai, to those interpreted for the conceptual model. In Figure 15, the model has a temperature of approximately 260^0C at an elevation of 600-700 masl. Moreover, at an elevation of 200 – 300 masl in the vicinity of KRC-B1, the model temperature is 220^0C. Also Figure 16 shows a comparable temperature distribution to the conceptual model. The temperatures ranging from 220^0 – 250^0 C at an elevation of 200 – 400 masl, near the Dua Belas Fault, are a good match to the temperatures shown in Figure 8.

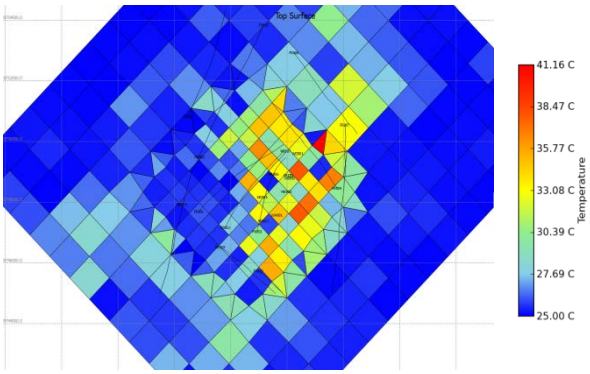

Figure 17: Surface temperatures in the model

Figure 17 shows that the surface temperature is elevated in some blocks where there are existing surface manifestations, but temperatures are lower than those measured. This can be explained by the fact that the model is built with a large block size, i.e., 500 m x 500 m. In most cases the area of hot springs and fumaroles is quite small, no more than approximately 10 m^2. Accordingly, the heat and mass flowing up to the surface is represented in the model as the average over both the surface feature and the surrounding cold terrain.

More details of the calibrated model are given by Prastika (2016).

4. FUTURE PRODUCTION

The future development of the Kerinci geothermal system is rather problematic due to the fact that the targeted potential areas are situated in the National Park Kerinci Seblat (NPKS). At present, it is impossible to have any drilling activities in that area due to restrictions, but it might be possible, in the future, that the regulator could allow exploration and exploitation that would not damage the park by setting up some compliance controls and regulations.

With this in mind three future scenarios were developed to investigate possible future production possibilities. For the first and second scenarios feedzone blocks were able to be located inside the National Park with the second scenario allowing more wells to be drilled. The last scenario had the restriction that the well pads must be located outside the National Park. As the third scenario is the most likely to be implemented, seven more cases (sub-scenarios) were investigated, with various well locations and different numbers of wells (see Prastika, 2016, for details).

Figure 18: Schedule of make-up wells for scenario SC-2 for two multipliers of the productivity indices (150 and 200)

In all cases the wells were run on deliverability so that the flow rate declined as the reservoir pressure dropped, with the rate of decline controlled by a productivity index (Pruess et al., 1999).

Unsurprisingly Scenario 2 was the most productive with 60 kg/s of steam being able to be sustained for 25 years using wells with a typical productivity index. With less wells Scenario 1 could sustain 50 kg/s for the same productivity index while the most productive case of Scenario 3 could only sustain 42 kg/s because of the limitations on well locations.

The most productive case within Scenario 3 (SC-2) was then used to investigate the development schedule that would be required to sustain 50 kg/s of steam production corresponding to 25 MW of electric power generation (see Prastika, 2016). Simulations were run using a range of productivity indices to determine the effect on the development schedule. The results shown in Figure 18 indicate that the target steam flow can be maintained, but only by drilling several make-up wells. Even for the high PI case (M200) 10 make-up wells are required over 25 years.

5. CONCLUSIONS

A conceptual model and then a natural state computer model of the undeveloped Kerinci geothermal field were presented. The study shows that despite the limited amount of geoscientific data and with no downhole well data a reasonable natural state model can be constructed. The model is constrained by the locations and magnitudes of the surface features which are able to be represented using the air-water equation-of-state.

The natural state model was used as the basis for a number of future scenario simulations. The results show that when well pads are restricted to locations outside the National Park, approximately 20 wells are required to maintain a production rate of 25 MWe. If the well pad locations are not restricted or deeper wells are able to be drilled then higher rates of production could be achieved or less wells would be required to sustain 25 MWe.

REFERENCES

Bellier, O., and Sébrier, M.: Is the slip rate variation on the Great Sumatran Fault accommodated by fore-arc stretching? *Geophysical Research Letters, 22*, 1969-1972 (1995).

Cumming, W.: Geothermal resource conceptual models using surface exploration data. *Proc. 34th Workshop on Geothermal Reservoir Engineering*. Stanford University, California: USA (2009).

Genrich, J.F. Bock, Y. McCaffrey, R. Prawirodirdjo, L. Stevens, C.W. Puntdewo, S.S.O. Subarya, C. & Wdowinski, S.: Distribution of slip at the northern Sumatra fault system, *Journal of Geophysical Research, 105*, 28.327-28.341 (2000).

Hasri, D. C.: *Review of Scientific Data from the Lempur Geothermal Prospect, Central Sumatra, Indonesia.* Geothermal Institute Project Report 84.12, University of Auckland, New Zealand (1984).

Hickman, R.G., Dobson, P.F., van Gerven, M., Sagala, B.D. & Gunderson, R.P.: Tectonic and stratigraphic evolution of the Sarulla graben geothermal area, North Sumatra, Indonesia, *Journal of Asian Earth Sciences, 23*, 435-448 (2004).

Hochstein, M.P., and Sudarman, S.: Geothermal resources of Sumatra, *Geothermics, 22*, 181-200 (1993).

JICA: *The Feasibility Study on Kerinci Geothermal Development Project in the Republic of Indonesia*. Final Report, Japan International Cooperation Agency, 236 p. (1989).

McCaffrey, R.: Slip vectors and stretching of the Sumatran fore arc, *Geology, 19*, 881-884 (1991).

McCaffrey, R., Zwick, P., Bock, Y., Prawirodirdjo, L., Genrich, J., Stevens, C.W., Puntodewo, S.S.O. & Subarya, C.: Strain partitioning during oblique plate convergence in northern Sumatra: Geodetic and seismologic constraints and numerical modelling, *Journal of Geophysical Research, 105*, 28, 363-28, 376 (2000).

O'Sullivan, M. J., Bullivant, D. P., Mannington, W. I., & Follows, S. E.: Modelling of the Wairakei – Tauhara geothermal system. *Proc. 20th New Zealand Geothermal Workshop*, University of Auckland, Auckland, New Zealand, 59-66 (1998).

Prastika, Y.: *Natural state model of Kerinci geothermal system, Jambi, Indonesia*. Master of Energy Report, University of Auckland (2016).

Prawirodirdjo, L., Bock, Y., Genrich, J.F., Puntdewo, S.S.O., Rais, J., Subarya, C. & Sutisna, S.: One century of tectonic deformation along the Sumatran fault from triangulation and Global Positioning System surveys, *Journal of Geophysical Research, 105*, 28.343-28.361, (2000).

Pruess, K., Oldenburg, C. & Moridis, G.: *TOUGH2 User's Guide, Version 2.0.* Lawrence Berkeley National Laboratory, Earth Sciences Division, Berkeley, California (1999).

Silitonga, H. T., Siahaan, E. E., Sasradipoera, D. S., Pelmelay, C. & Timisela, D. P.: Exploration Strategy in Kerinci Geothermal Prospect located inside the National Park of Indonesia. *Proc. World Geothermal Congress 2015*. Melbourne, Australia (2015).

Utami, P.: *Geothermal Geology*. Unpublished lectures note, University of Auckland, New Zealand (2015).

Yeh, A., Croucher, A. & O'Sullivan, M.: Recent Developments in the AUTOUGH2 Simulator. *Proc. TOUGH Symposium 2012*, Berkeley, California, USA (2012).

Yeh, A., Croucher, A. E. & O'Sullivan, M.: TIM-Yet another graphical tool for TOUGH2. *Proc. 35th New Zealand Geothermal Workshop*, Rotorua, New Zealand (2013).